Journal of Materials Chemistry A

Accepted Manuscript

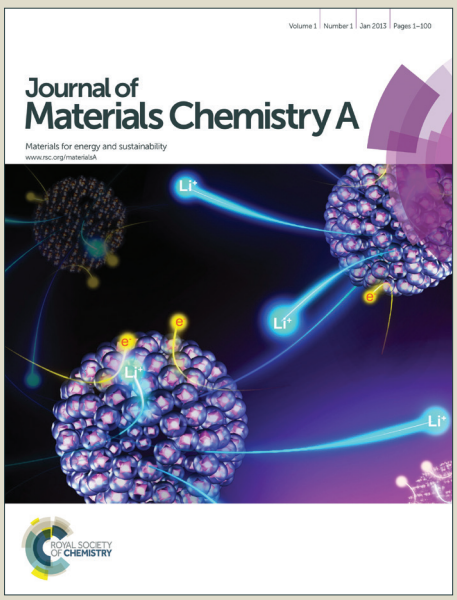

ROYAL SOCIETY OF CHEMISTRY

www.rsc.org/materialsA

Cite this: DOI: 10.1039/c0xx00000x

www.rsc.org/xxxxxx

ARTICLE TYPE

Enhanced rate capability and cycle stability of lithium-sulfur batteries with a bifunctional MCNT@PEG-modified separator

Guanchao Wang[a], Yanqing Lai[a], Zhian Zhang[a*], Jie Li[a], Zhiyong Zhang[a]

Received (in XXX, XXX) Xth XXXXXXXXX 20XX, Accepted Xth XXXXXXXXX 20XX

DOI: 10.1039/b000000x

As one of the most promising high-energy lithium batteries, the commercialization of Lithium-sulfur (Li-S) batteries remains a huge challenge due to their poor rate performance and low cycle stability, which are partly originated from the dissolution of polysulfides and their migration from S cathode to the Li anode through the separator. While novel sulfur-based composite cathodes have been put forward constantly to restraint the dissolution of polysulfides, less attention has been paid to modifying the separator. In this work, a multi-walled carbon nanotube@polyethylene glycol (MCNT@PEG) composite is designed and prepared to modify the commercial Celgard separator. With the bifunctional MCNT@PEG-modified separator, Li-S cells possess a high initial discharge capacity of 1283 mAh g^{-1} at 0.5 C and undertake a long charge/discharge process of 500 cycles at 1 C, with 0.12% capacity fading per cycle. Moreover, even the rate is increased to 5 C, the cells can also deliver a discharge capacity of 657 mAh g^{-1}. These encouraging electrochemical results demonstrate excellent rate capability and high cycle stability of Li-S cells, which could be attributed to the strong chemical and physical absorption properties and high electron conductivity of the MCNT@PEG layer. This facile approach to restrain the shuttle effect of polysulfides makes further progress to obtain enhanced performance of Li-S batteries.

Introduction

Rechargeable lithium batteries with a long charge/discharge life and high energy density are urgently needed for satisfying the continuously accelerating requirements of portable electronics and electric vehicles (EV)[1, 2].Lithium-sulfur (Li-S) batteries have particularly attracted attention among the various rechargeable battery systems on account of their high theoretical energy density (2600 Wh kg^{-1}) and specific capacity (1675 mAh g^{-1}). In addition, sulfur takes the advantages of abundance in nature, low cost and environmental friendliness[3-5]. However, the practical energy density of Li-S batteries are hindered by their poor rate performance and low cycle stability, which are mainly originated from the dissolution of polysulfides and their migration from S cathode to the Li anode through the separator[6, 7]. Polysulfides (Li_2S_x, $4<x\leq8$) are generated as intermediate products during the charge/discharge processes, which are soluble in organic electrolyte, resulting in the shuttle effect between the cathode and anode[8-11].

To overcome the intractable shuttle effect of Li-S batteries, novel S cathodes and cell configurations are put forward[12, 13]. For the S cathodes, porous carbon structures[14-16], porous metal oxides[17] and conductive polymers[18, 19] have been employed to enhance the conductivity of the S cathodes and confine the S within the cathode region. These methods have shown a significant improvement of the electrochemical performance of Li-S batteries. However, the introduction of novel structures often involves complex manufacturing processes and lowers the sulfur content in the cathode[20]. The configuration modification of Li-S batteries is another promising strategy for enhancing electrochemical performance. Recently, an interlayer between the cathode and separator functioning as a polysulfide barrier has been proved to substantially improve the energy density and cycle stability of Li-S batteries[21, 22]. Nevertheless, the insertion with a thick interlayer is adverse to the improvement of energy density. In addition, the fabrication of the interlayer could be complicated.

The separator, which keeps free ionic pathway and blocks the transport of electrons across the cathode and anode, is a critical component part of Li-S batteries. Recently, metal oxides[23, 24], polymers[25-27] and conductive carbon materials[28-30] have been adopted to modify the separator of Li-S batteries, which can facilitate the adsorption and trapping of soluble polysulfides and ensure good electrolyte immersion and penetration. However, previous researchers almost concentrate on the physically absorption of the polysulfides, rarely attention is paid to chemical absorption of polysulfides. PEG is usually employed to cathode composites to restrain the polysulfides diffusing from cathode to anode, which provides hydrophilic groups and enhances the Li^+ ion transport[31-33]. In this work, a strategy of combining physical and chemical adsorption of polysulfides was proposed to restrain the polysulfides shuttle. Moreover, different from those of other materials modified with PEG through simple mixing, a novel composite with polyethylene glycol (PEG) grafted on the multi-walled carbon nanotube (MCNT) is designed and synthesized. Subsequently, the composite is coated onto one side of the commercial separator with a slurry-coated method. With the

MCNT@PEG-modified separator, the Li-S cells possess a high initial discharge capacity of 1283 mAh g^{-1} at 0.5 C and undertake a long charge/discharge process of 500 cycles at 1 C, with 0.12% capacity fading per cycle. Noteworthily, even the rate is increased to 5 C, the cells can also deliver a discharge capacity of 657 mAh g^{-1}.These encouraging electrochemical performances exhibited excellent rate capability and high cycle stability of Li-S cells, indicating the MCNT@PEG-modified separator has a great potential in the applications of Li-S batteries.

Experimental

Materials preparation

First, 1.0 g MCNTs (Aladdin reagent, 10 to 20 nm in diameter, 2% carboxylic) were added in a 100 mL Teflon-lined stainless steel autoclave, where 10 mL concentrated HNO_3 was added previously. Then, the autoclave was taken to 170 °C oven for 2 h. Afterwards, the obtained functionalized MCNTs (f-MCNTs) were washed to a neutral PH and dried at 60 °C for 6 h; Subsequently, 0.1 g PEG-10000 (Aladdin reagent) and 0.5 g f-MCNTs were dispersed into a solution, which consisted of 200 mL deionized water and 10 mL concentrated H_2SO_4. Then the mixture was magnetically stirred at 60 °C for 24 h to ensure the carboxylic groups of f-MCNTs and the hydroxyl groups of PEG reacted with completely. Finally, the obtained MCNT@PEG composite was washed three times with deionized water, and then dried under vacuum at 60 °C for 6 h.

A slurry method was adopted to coat the separator with the MCNT@PEG composite. A mixture of MCNT@PEG composite and polyvinylidene fluoride (PDVF) (9:1, by mass) was mixed with N-methylpyrrolidinone (NMP, Sigma Aldrich) to form slurry, which was coated on one side of the Celgard 2400 separator. Then the MCNT@PEG-modified separator was dried under vacuum at 50 °C for 6 hours.

Material characterization

Field emission scanning electron microscopy (SEM, Nova Nano SEM 230) and transmission electron microscopy (TEM, Tecnai G2 20ST) were employed to characterize the morphology. The elements on the surface of sample were identified by energy-dispersive X-ray spectroscopy (EDS). Fourier transformation infrared spectroscopy (FTIR) was obtained by an infrared spectrometer (Nicolet 6700, USA) with KBr plate.

Electrochemical measurements

The S cathode was fabricated by a slurry coating method. The composite cathode slurry was composed of S, acetylene black and polyvinylidene fluoride (PVDF) dissolved in N-methyl pyrrolidinone (NMP) at the weight ratio of 60: 30: 10. The slurry of the cathode was coated onto an aluminium foil with a doctor blade, dried under vacuum at 60 °C for 12 h. The mass loading of active material sulfur is about 1.60 mg cm^{-2}.The electrolyte was made up of 1 M bis(trifluoromethane) sulfonamide lithium salt (LiTFSI, Sigma Aldrich) dissolved in a mixture of 1,3-dioxolane (DOL, Acros Organics) and 1,2-dimethoxyethane (DME, Acros Organics) (1: 1, by volume), with 0.1 M $LiNO_3$ as an electrolyte additive. Lithium sheet was used as counter electrode and the MCNT@PEG-modified Celgard 2400 was used as separator.

Results and discussion

Fig. 1 describes the cell configuration with the MCNT@PEG-modified separator, where the coating is faced to the sulfur cathode, acting for intercepting the migrating polysulfides and working as a conductive upper current collector to accelerate the transport of electron[34]. On the other hand, the way that PEG grafted on the MCNTs ensures excellent mechanical strength, thus guaranteeing its normal functions during cell fabrication and charge/discharge process[35].

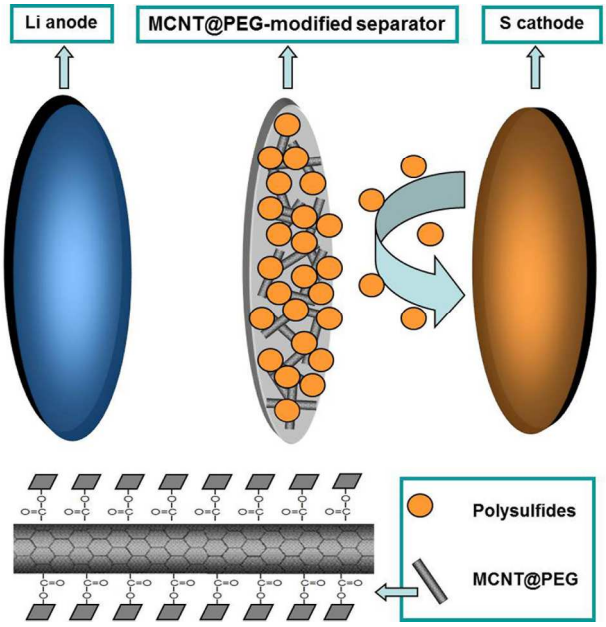

Fig. 1 The schematic of a Li-S cell configuration with a MCNT@PEG-modified separator.

The surface morphology of the Celgard separator of the MCNT@PEG-modified separator is exhibited in Fig. 2(a). The Celgard separator presents a uniformly reticular structure which keeps free ionic pathway and blocks the transport of electrons across the cathode and anode[27]. Fig. 2(b) presents the sectional view of the MCNT@PEG-modified separator, demonstrating the close attachment between the Celgard separator and the MCNT@PEG layer. The thickness and weight of the MCNT@PEG coating are about 6.70 μm and 0.26 mg cm^{-2}, by contrast, the Celgard 2400 separator are about 19.23 μm in thickness and 1.20 mg cm^{-2} in weight. The scanning electron microscopy (SEM) image and the corresponding energy-dispersive X-ray spectroscopy (EDX) elemental mapping of the MCNT@PEG-modified separator before and after 100 cycles at 1 C is shown as in Fig. 2(c) and Fig. 2(d). It can be seen that the coating layer consists of interwoven and curved MCNT@PEG composite, which acts as a filter on the Celgard separator. This filter with uneven surface and porous structure is essential for absorbing polysulfides[34]. EDX inspection of the MCNT@PEG-modified separator before cycles shows no elemental sulfur is detected, while after cycles clear elemental sulfur (marked as yellow) is uniformly distributed in the carbon matrix (marked as red), evidencing the interception and absorption properties of the MCNT@PEG composite[36].

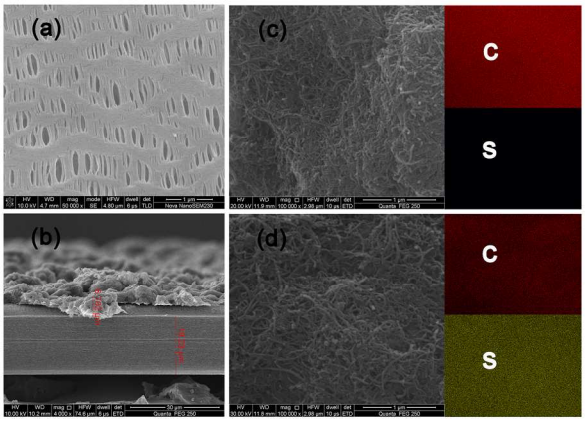

Fig. 2 SEM images of the Celgard separator (a) and a typical sectional view of the MCNT@PEG-modified separator (b). SEM images and elemental mapping of the MCNT@PEG-modified separator before cycles (c) and after 100 cycles at 1 C (d).

To further identify the microstructure of the MCNT@PEG composite, transmission electron microscopy (TEM) images are investigated. As illustrated in Figure. 3(a) and (b), most of the nanotubes connect with each other into a sparse net, guaranteeing a good electron pathway. Figure. 3(c) and (d) indicate that a rough and porous film is uniformly coated on the surface of the MCNTs, revealing the presence of PEG.

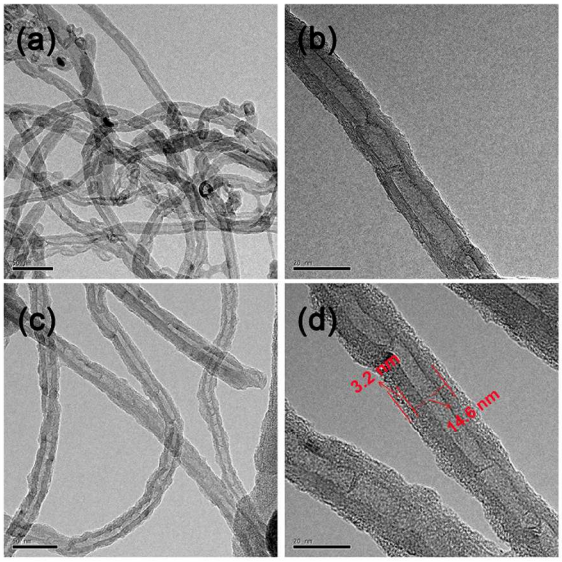

Fig. 3 TEM observation of the MCNTs (a and b), TEM observation of the MCNT@PEG composite (c and d).

PEG is also confirmed to graft on the surface of MCNTs by FTIR spectra as presented in Fig. 4. C=C and C-OH bands are detected in the FTIR spectra of MCNT, f-MCNT and MCNT@PEG, respectively, at 1575 cm^{-1} and 1213 cm^{-1}. The C=OOH band (1723 cm^{-1}) of f-MCNT becomes a broader C=OOR band of MCNT@PEG and shifts from 1702 cm^{-1} to 1718 cm^{-1}. The changes shown in FTIR spectra result from the reaction of the carboxylic groups of the MCNT with the hydroxyl groups of the PEG[35]. Accordingly, the special structure obtained could make full use of the advantage of MCNTs and PEG, physically and chemically restraining polysulfides shuttle and providing channel for Li^+ and electron transport[37]. Such an optimized electrochemical environment ensures efficient sulfur utilization and high reversibility.

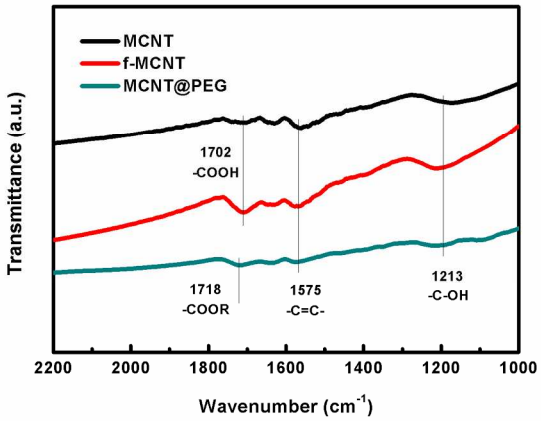

Fig. 4 FTIR spectra of the MCNT, f-MCNT and MCNT@PEG composite.

In order to demonstrate the possible advantages of MCNT@PEG-modified separator, the electrochemical performance was tested by galvanostatic charge/discharge in a coin cell. Fig. 5(a) shows the charge/discharge curves of the cells with the MCNT@PEG-modified separator at a current density of 0.5 C. The upper discharge plateau at 2.3 V shows a rapid kinetic process of the conversion of sulfur to long-chain polysulfides (Li_2S_x, $4<x\leq8$). The lower discharge plateau at 2.1 V shows a strong reduction of long-chain soluble polysulfides to insoluble low-order Li_2S_2, and eventually, to Li_2S. During the process of charge, the two continuous charge plateaus at 2.2 and 2.4 V represent the oxidation reactions of Li_2S_2/Li_2S to Li_2S_8/S[38]. The overlapping charge/discharge indicating limited polysulfides fusion and active material loss. On the other hand, it also demonstrates that the MCNT@PEG coating can significantly restrain the diffusion of polysulfides into the electrolyte from cathode to anode and reactivate the trapped active material, ensuring the high reversibility and stability of the cell. Cyclic voltammogram (CV) curves at 0.2 mV s^{-1} of the Li-S cells with the MCNT@PEG-modified separator during the first five cycles are presented in Fig. 5(b), from which the typical two-step reduction reactions in the cathodic sweep and two overlapping oxidation reactions in the anodic sweep, consistent well with the current peaks in the discharge/charge curves. The CV curves maintain a good overlap, indicating that the cells with MCNT@PEG-modified separator have an excellent reversible capacity and high cycle stability[39].

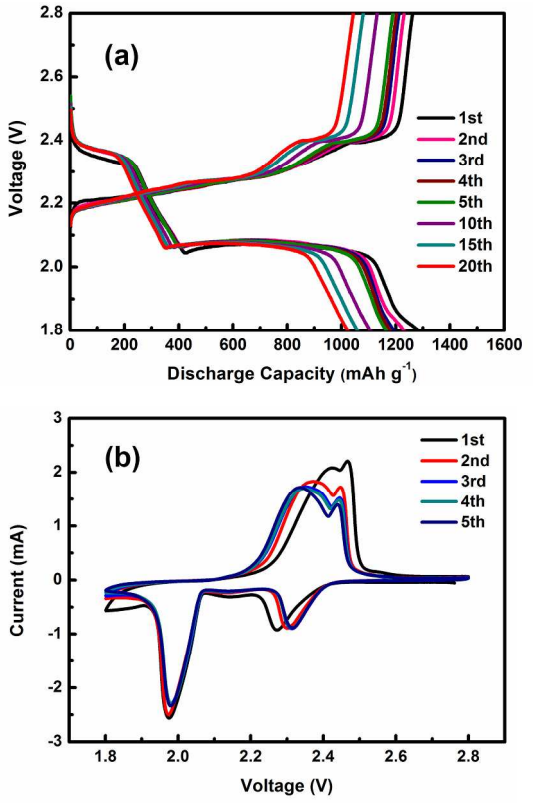

Fig. 5 Electrochemical analyses of the Li-S batteries with the MCNT@PEG-modified separator: Discharge/charge curves (a) and CV curves at 0.2 mV s^{-1} (b).

Figure. 6(a) demonstrates the cycle performance of the Li-S cells with the MCNT@PEG-modified separator at 0.5 C, 1 C, 2 C and 5 C. After utilizing the MCNT@PEG-modified separator, the initial discharge capacities of the cell reach to 1283, 1250, 1215 and 1022 mAh g^{-1} at 0.5 C, 1 C, 2 C and 5 C, respectively. In the process of charge/discharge, the MCNT@PEG-modified separator allows the cell to function normally, suppresses the diffusion of polysulfides and offers efficient electron conduction and fast ion transport. Therefore, the cells with the MCNT@PEG-modified separator exhibit excellent capacity retention of 727, 637, 558 and 526 mAh g^{-1} at 0.5 C, 1 C, 2 C and 5 C after 200 cycles, respectively. Thus, at various rate, the MCNT@PEG-modified separator greatly lowers the capacity fading to 0.22%, 0.25%, 0.27% and 0.24% per cycle.

The rate capability of the cell with the MCNT@PEG-modified separator is further investigated by cycling at elevated charge/discharge rates from 0.2 C to 5 C. The discharge capacities at different rates are presented in Fig. 6(b). During the first 5 cycles, the reversible capacity fades with time at 0.2 C and retains a capacity of 1176 mAh g^{-1}. At a higher rate of 0.5 C, a capacity of 998 mAh g^{-1} is delivered. Further the current density is increased to 1 C and 2 C, a discharge capacity of 876 mAh g^{-1} and 769 mAh g^{-1} is reached, respectively. Particularly, even the current density is increased to 5 C, the cells also remain the capacity of 657 mAh g^{-1}. When the rate is back to 0.5 C, a reversible capacity of 893 mAh g^{-1} is recovered. Moreover, the capacities of the cells also demonstrate high stability at varying rate from 0.2 C to 5 C. The excellent rate capability can be owing to the excellent electron conductivity and strong physical and chemical polysulfides absorption of the MCNT@PEG composite.

As shown in Fig. 6(c), long-term charge/discharge cycling is tested for the cells with the MCNT@PEG-modified separator, MCNT-modified separator and Celgard separator at a 1 C rate. The cell with the MCNT@PEG-modified separator exhibits high cycle stability, achieving 490 mAh g^{-1} after 500 cycles. In contrast, the cell with MCNT-modified separator and Celgard separator can only deliver the capacity of 335 and 129 mAh g^{-1}, respectively. That is to say, the capacity retention of the cell increases from 17.5% to 39.2% after adopting the MCNT@PEG-modified separator. Moreover, with the MCNT@PEG-modified separator, the cell shows a more significant polysulfide-trapping capability than the MCNT-modified separator, suggesting that the combination of physical and chemical polysulfides absorption is an effective method to obtain better electrochemical performance of Li-S cells. These results demonstrate that the MCNT@PEG-modified separator could significantly restraint the diffusion of polysulfides, promoting reversible capacity and improving the cycling performance of the Li-S cells.

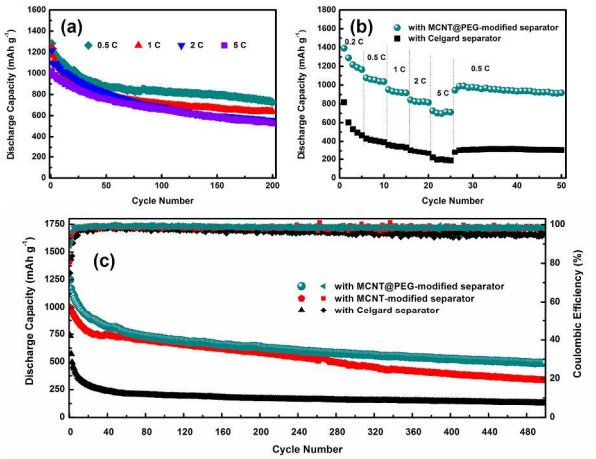

Fig. 6 Cycling performance of the Li-S batteries with the MCNT@PEG-modified separator at various rates of 0.5 C, 1 C, 2 C and 5 C (a); Rate performance of the Li-S batteries with the MCNT@PEG-modified separator (b); long-term cycling performance of Li-S batteries with the MCNT@PEG-modified separator, MCNT-modified separator and commercial Celgard separator at a 0.5 C rate (c).

Electrochemical impedance spectra of the cell with the MCNT@PEG-modified separator and commercial Celgard separator before cycling are shown in Fig. 7 with frequency from 0.01 Hz to100 kHz . As Fig. 7 illustrated, the Nyquist plots of cell before discharge consist of a semicircle at high frequency and medium frequency and an inclined line at low frequency, in accordance with the precedent researches[40, 41]. The intercept at high frequency on the real axis indicates the ohmic resistance (R_O). At high frequency to medium frequency, the charge transfer resistance (R_{ct}) is represented by the diameter of the semicircle, which comes from the interface of the electrolyte and the electrode. Besides, the inclined line at low frequency corresponds to Warburg impedance (Wo). Base on the equivalent circuit fitting, the charge transfer resistance (R_{ct}) decreases from 59.41 Ω to 23.5 Ω after using the MCNT@PEG-modified separator

instead of Celgard separator. The reduction in R_{ct} can be attributed to the excellent utilization of the active material, the higher electrolyte retention and the excellent conductivity of electrons, leading to the rapid and abundant reaction of Li^+ and active material. Furthermore, the results in cycle performance and rate capacity test indicate that the cell with the MCNT@PEG-modified separator exhibits a higher reversible capacity and a better rate capability than the cell with the Celgard separator, in accordance with the impedance result, which is similar to the phenomenon found in other works[42, 43].

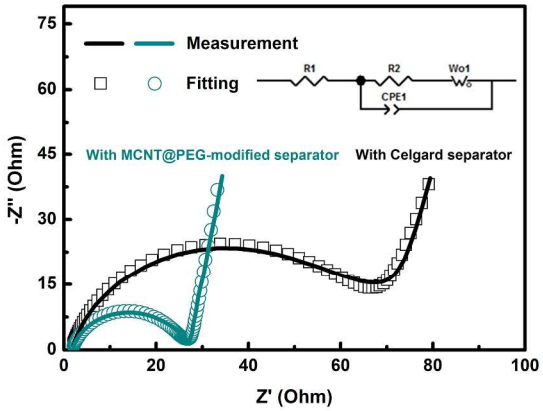

Fig. 7 Nyquist plots and the equivalent circuit of the cell with the MCNT@PEG-modified separator and commercial Celgard separator before cycles.

The optical images comparison of polysulfides diffusion between the Celgard separator and MCNT@PEG-modified separator is presented in Fig. 8, in which polysulfides of the same concentration are distributed in DME: DOL mixture. As it can be seen, the MCNT@PEG-modified separator expresses a preferable inhibition of polysulfides diffusion from the Celgard separator. After 10, 30 and 120 minutes of rest, the electrolyte with Celgard separator turns brown obviously, while the electrolyte with MCNT@PEG-modified separator shows a slight change in colour, showing a positive suppression of the diffusion of polysulfides. The phenomenon can be ascribed to the excellent chemical and physical polysulfides absorption capability of MCNT@PEG composite, thus the polysulfides traverse the separator with more obstructions. Accordingly, the outstanding electrochemical performance of the MCNT@PEG-modified separator is authenticated.

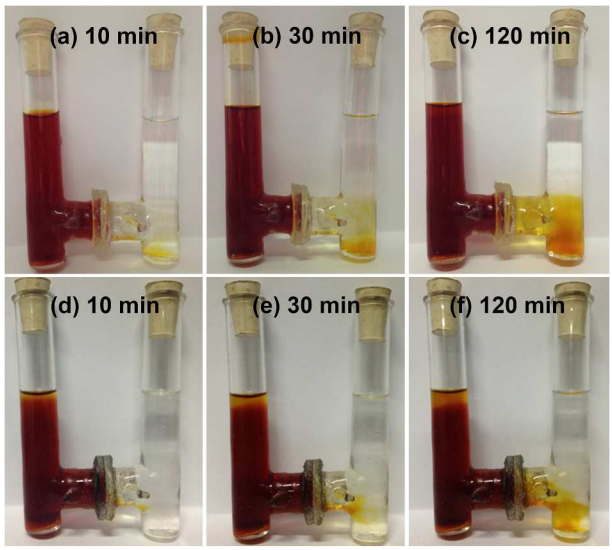

Fig. 8 The optical images of the diffusion of polysulfides of Celgard separator (a-c) and MCNT@PEG-modified separator (d-f) toward different resting times.

Conclusion

A novel MCNT@PEG composite is synthesized by a simple method and coated on the commercial Celgard separator. With the MCNT@PEG-modified separator, Li-S cells deliver a high initial discharge capacity (1283 mAh g^{-1}), a long cycle life (500 cycles), and high reversibility (0.12% capacity fading per cycle). The enhanced electrochemical performance ascribes that the MCNT@PEG coating serves as a conductive upper current collector, physically and chemically restraining polysulfides shuttle and providing channel for ion and electron transport. This method of separator surface modification opens a new approach for Li-S batteries with excellent performance.

Acknowledgements

The authors acknowledge the financial support of the Teacher Research Fund of Central South University (2013JSJJ027) and the Natural Science Foundation of China (51474243).

Notes and references

[a] *School of Metallurgy and Environment, Central South University, Changsha 410083, China*
** E-mail address: zza75@163.com*

1. R. J. Chen, T. Zhao and F. Wu, *Chem Commun.*, 2015, **51**, 18-33.
2. L. Sun, W. Kong, Y. Jiang, H. Wu, K. Jiang, J. Wang and S. Fan, *J. Mater. Chem. A*, 2014, DOI: 10.1039/c4ta06255h.
3. Z. Yuan, H. J. Peng, J. Q. Huang, X. Y. Liu, D. W. Wang, X. B. Cheng and Q. Zhang, *Adv. Funct. Mater.*, 2014, **24**, 6105-6112.
4. J. Song, Z. Yu, T. Xu, S. Chen, H. Sohn, M. Regula and D. Wang, *J. Mater. Chem. A*, 2014, **2**, 8623-8627.
5. G. Zhou, L. Li, C. Ma, S. Wang, Y. Shi, N. Koratkar, W. Ren, F. Li and H. M. Cheng, *Nano Energy*, 2015, **11**, 356-365.
6. Y. X. Yin, S. Xin, Y. G. Guo and L. J. Wan, *Angew. Chem. Int. Ed. Engl.*, 2013, **52**, 13186-13200.
7. G. Xu, B. Ding, J. Pan, P. Nie, L. Shen and X. Zhang, *J. Mater. Chem. A*, 2014, **2**, 12662-12676.
8. K. Zhang, Q. Li, L. Zhang, J. Fang, J. Li, F. Qin, Z. Zhang and Y. Lai, *Mater. Lett.*, 2014, **121**, 198-201.

9. L. X. Miao, W. K. Wang, K.G. Yuan, Y. S. Yang and A. B. Wang, *Chem Commun.*, 2014, **50**, 13231-13234.
10. S. S. Zhang, *J. Power Sources*, 2013, **231**, 153-162.
11. A. Manthiram, Y. Fu, S. H. Chung, C. Zu and Y. S. Su, *Chem. Rev.*, 2014, **114**, 11751-11787.
12. Z. Lin, C. D. Liang, *J. Mater. Chem. A*, 2015, **3**, 936-958.
13. D. W. Wang, Q. Zeng, G. Zhou, L. Yin, F. Li, H. M. Cheng, I. R. Gentle and G. Q. M. Lu, *J. Mater. Chem. A*, 2013, **1**, 9382-9394.
14. S. Xin, L. Gu, N. H. Zhao, Y. X. Yin, L. J. Zhou, Y. G. Guo and L. J. Wan, *J. Am. Chem. Soc.*, 2012, **134**, 18510-18513.
15. S. Zhao, C. Li, W. Wang, H. Zhang, M. Gao, X. Xiong, A. Wang, K. Yuan, Y. Huang and F. Wang, *J. Mater. Chem. A*, 2013, **1**, 3334-3339.
16. X. B. Cheng, J. Q. Huang, Q. Zhang, H. J. Peng, M. Q. Zhao and F. Wei, *Nano Energy*, 2014, **4**, 65-72.
17. Z. Wei Seh, W. Li, J. J. Cha, G. Zheng, Y. Yang, M. T. McDowell, P. C. Hsu and Y. Cui, *Nat Commun*, 2013, **4**, 1331-1336.
18. W. Zhou, Y. Yu, H. Chen, F. J. DiSalvo and H. D. Abruna, *J. Am. Chem. Soc.*, 2013, **135**, 16736-16743.
19. G. Ma, Z. Wen, J. Jin, Y. Lu, X. Wu, C. Liu and C. Chen, *RSC Advances*, 2014, **4**, 21612-21618.
20. S. H. Chung and A. Manthiram, *Adv. Funct. Mater.*, 2014, **24**, 5299-5306.
21. G. Ma, Z. Wen, J. Jin, M. Wu, X. Wu and J. Zhang, *J. Power Sources*, 2014, **267**, 542-546.
22. S. H. Chung and A. Manthiram, *Chem Commun.*, 2014, **50**, 4184-4187.
23. Z. Zhang, Y. Lai, Z. Zhang, K. Zhang and J. Li, *Electrochim. Acta*, 2014, **129**, 55-61.
24. W. Li, J. Hicks-Garner, J. Wang, J. Liu, A. F. Gross, E. Sherman, J. Graetz, J. J. Vajo and P. Liu, *Chem. Mater.*, 2014, **26**, 3403-3410.
25. S. S. Zhang and D. T. Tran, *J. Mater. Chem. A*, 2014, **2**, 7383-7388.
26. I. Bauer, S. Thieme, J. Brückner, H. Althues and S. Kaskel, *J. Power Sources*, 2014, **251**, 417-422.
27. J. Q. Huang, Q. Zhang, H. J. Peng, X. Y. Liu, W. Z. Qian and F. Wei, *Energy Environ. Sci.*, 2014, **7**, 347-353.
28. H. B. Yao, K. Yan, W. Y. Li, G. Y. Zheng, D. S. Kong, Z. W. She, V. K. Narasimhan, Z. Liang and Y. Cui, *Energy Environ. Sci.*, 2014, **7**, 3381-3390.
29. Y. S. Su and A. Manthiram, *Chem Commun.*, 2012, **48**, 8817-8819.
30. A. Vizintin, M. U. M. Patel, B. Genorio and R. Dominko, *ChemElectroChem*, 2014, **1**, 1040-1045.
31. F. Sun, J. Wang, H. Chen, W. Li, W. Qiao, D. Long and L. Ling, *Appl. Mater. Interfaces*, 2013, **5**, 5630-5638.
32. S. M. Zhang, Q. Zhang, J. Q. Huang, X. F. Liu, W. Zhu, M. Q. Zhao, W. Z. Qian and F. Wei, *Part. Part. Syst. Charact*, 2013, **30**, 158-165.
33. Z. Li, L. Yuan, Z. Yi, Y. Liu, Y. Xin, Z. Zhang and Y. Huang, *Nanoscale*, 2014, **6**, 1653-1660.
34. S. H. Chung and A. Manthiram, *J. Phys. Chem. Lett.*, 2014, **5**, 1978-1983.
35. L. X. Miao, W. K. Wang, A. B. Wang, K. G. Yuan and Y. S. Yang, *J. Mater. Chem. A*, 2013, **1**, 11659-11664.
36. S. H. Chung and A. Manthiram, *Adv. Mater.*, 2014, **26**, 7352-7357.
37. J. Q. Huang, Q. Zhang, S. M. Zhang, X. F. Liu, W. Zhu, W. Z. Qian and F. Wei, *Carbon*, 2013, **58**, 99-106.
38. Q. Li, Z. Zhang, K. Zhang, J. Fang, Y. Lai and J. Li, *J. Power Sources*, 2014, **256**, 137-144.
39. S. H. Chung and A. Manthiram, *Adv. Mater.*, 2014, **26**, 1360-1365.
40. H. Wei, J. Ma, B. Li, Y. Zuo and D. Xia, *Appl. Mater. Interfaces*, 2014, **6**, 20276-20281.
41. Z. Deng, Z. Zhang, Y. Lai, J. Liu, J. Li and Y. Liu, *J. Electrochem. Soc.*, 2013, **160**, A553-A558.
42. X. Liu, Z. Shan, K. Zhu, J. Du, Q. Tang and J. Tian, *J. Power Sources*, 2015, **274**, 85-93.
43. G. Zhou, S. Pei, L. Li, D. W. Wang, S. Wang, K. Huang, L. C. Yin, F. Li and H. M. Cheng, *Adv. Mater.*, 2014, **26**, 625-631.

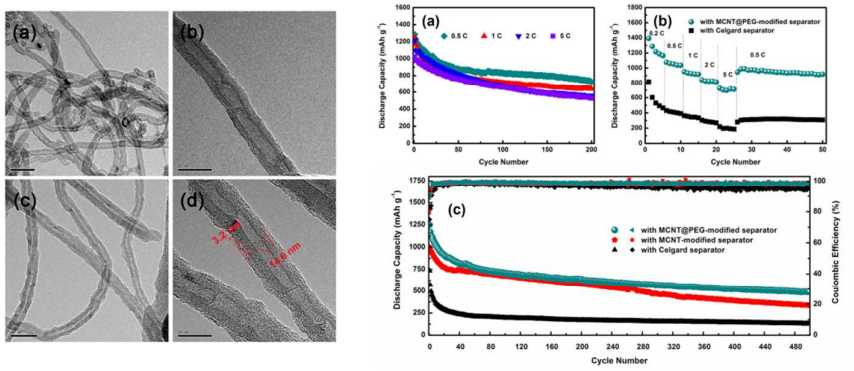

A multi-walled carbon nanotube@polyethylene glycol (MCNT@PEG) composite is designed and prepared to modify the commercial Celgard separator. With the bifunctional MCNT@PEG-modified separator, Li-S cells possess a high initial discharge capacity of 1283 mAh g^{-1} at 0.5 C and undertake a long charge/discharge process of 500 cycles at 1 C, with 0.12% capacity fading per cycle. Moreover, even the rate is increased to 5 C, the cells can also deliver a discharge capacity of 657 mAh g^{-1}. These encouraging electrochemical results demonstrate excellent rate capability and high cycle stability of Li-S cells, which could be attributed to the strong chemical and physical absorption properties and high electron conductivity of the MCNT@PEG layer.